THE JOURNAL OF BIOLOGICAL CHEMISTRY VOL. 283, NO. 40, pp. 26956–26964, October 3, 2008
Printed in the U.S.A.

An Iron Responsive Element-like Stem-Loop Regulates α-Hemoglobin-stabilizing Protein mRNA*[S]

Received for publication, March 28, 2008, and in revised form, July 18, 2008 Published, JBC Papers in Press, August 2, 2008, DOI 10.1074/jbc.M802421200

Camila O. dos Santos[‡], Louis C. Dore[‡], Eric Valentine[‡], Suresh G. Shelat[§], Ross C. Hardison[¶], Manik Ghosh[‖], Wei Wang[**], Richard S. Eisenstein[‡‡], Fernando F. Costa[§§], and Mitchell J. Weiss[‡1]

*From the [‡]Division of Hematology and [§]Department of Pathology & Laboratory Medicine, Children's Hospital of Philadelphia, Philadelphia, Pennsylvania 19104, the [¶]Department of Biochemistry and Molecular Biology, Center for Comparative Genomics and Bioinformatics, Pennsylvania State University, University Park, Pennsylvania 16802, the [‖]Cell Biology and Metabolism Branch, NICHD, National Institutes of Health, Bethesda, Maryland 20892, the **Department of Biochemistry,Wake Forest University Health Sciences, Winston-Salem, North Carolina 27157, the [‡‡]Department of Nutritional Sciences,University of Wisconsin, Madison, Wisconsin 53706, and the [§§]Center of Hemotherapy and Hematology, State University of Campinas, Sao Paulo, Brazil*

Hemoglobin production during erythropoiesis is mechanistically coupled to the acquisition and metabolism of iron. We discovered that iron regulates the expression of α-hemoglobin-stabilizing protein (AHSP), a molecular chaperone that binds and stabilizes free α-globin during hemoglobin synthesis. In primates, the 3′-untranslated region (UTR) of *AHSP* mRNA contains a nucleotide sequence resembling iron responsive elements (IREs), stem-loop structures that regulate gene expression post-transcriptionally by binding iron regulatory proteins (IRPs). The *AHSP* IRE-like stem-loop deviates from classical consensus sequences and binds IRPs poorly in electrophoretic mobility shift assays. However, in cytoplasmic extracts, *AHSP* mRNA co-immunoprecipitates with IRPs in a fashion that is dependent on the stem-loop structure and inhibited by iron. Moreover, this interaction enhances *AHSP* mRNA stability in erythroid and heterologous cells. Our findings demonstrate that IRPs can regulate mRNA expression through non-canonical IREs and extend the repertoire of known iron-regulated genes. In addition, we illustrate a new mechanism through which hemoglobin may be modulated according to iron status.

Hemoglobin (Hb)[2] is a heterotetramer composed of α- and β-globin polypeptides, each bound to a heme prosthetic group consisting of protoporphyrin IX complexed to iron. Free globins, heme synthetic intermediates and iron are all cytotoxic. Accordingly, numerous mechanisms have evolved to coordinate Hb synthesis and limit the damage caused by its individual components. Iron is of particular concern, because it catalyzes the formation of reactive oxygen species (ROS) that chemically alter proteins, lipids, and nucleic acids.

Under normal circumstances, most circulating iron is bound by transferrin, which is internalized by specific receptors on the plasma membrane of most cells. Iron uptake in erythroid precursors is modulated by availability of transferrin-bound iron, the number of functional transferrin receptors (TFR1) on the cell surface, and in iron-overload states, nontransferrin-bound iron (1). Like most other cells, erythroid precursors regulate iron through the coordinated synthesis of TFR1 and the intracellular iron storage protein ferritin via an iron sensor system consisting of iron responsive elements (IRE) and iron regulatory proteins (IRP1 and IRP2) (reviewed in Refs. 2–4). Iron responsive elements are present in mRNA UTRs and form stem-loop structures that are recognized by iron-sensing IRPs. Increased iron and/or heme levels regulate IRP activities. Insertion of an [4Fe-4S] iron-sulfur cluster into IRP1 inhibits its RNA binding activity and converts the protein to the cytosolic aconitase (5). In contrast, iron stimulates proteosomal degradation of IRP2 (6, 7), though a mechanism that may involve binding to heme (8–10). Binding of IRPs to 5′-UTR IREs inhibits its mRNA translation while IRP/IRE interactions within the 3′-UTR enhance transcript stability by protecting from endonuclease degradation (11). The stability of *TFR1* mRNA is regulated by multiple IREs within the 3′-UTR(12, 13). In contrast, *CDC14A* and *SLC11A2/DMT1* mRNAs contain single functional IREs within their 3′-UTRs (14, 15).

In addition to utilizing the generalized IRE system, erythroid cells contain mechanisms that link globin synthesis to iron availability. For example, iron promotes globin production by regulating activity of the heme-regulated inhibitor kinase, HRI, which inactivates the general translation initiation factor elF2 (16). Heme, which is produced when iron is replete, binds and inactivates HRI, enhancing globin translation. Iron deficiency depletes heme, thereby activating HRI to inhibit globin protein synthesis. Iron also regulates globin gene transcription via the nuclear heme-binding protein, Bach1. In the absence of heme,

* This work was supported, in whole or in part, by National Institutes of Health Grants R01 DK61692 and R01 HL087427 (to M. J. W.), R01 DK65806 (to R. C. H.), and R01 DK66600 (to R. S. E.). This work was also supported by an American Heart Association Postdoctoral Fellowship Award (Grant 4247620608) (to C. O. S.), by Fundação de Amparo à Pesquisa do Estado de São Paulo (FAPESP) (Grant 02/13801–7) (to F. F. C.). The costs of publication of this article were defrayed in part by the payment of page charges. This article must therefore be hereby marked "*advertisement*" in accordance with 18 U.S.C. Section 1734 solely to indicate this fact.

[S] The on-line version of this article (available at http://www.jbc.org) contains supplemental Tables S1 and S2.

[1] A Leukemia and Lymphoma Society Scholar. To whom correspondence should be addressed: Children's Hospital of Philadelphia, Division of Hematology, 3615 Civic Center Blvd., Philadelphia, PA 19104. Tel.: 215-590-0565; Fax: 215-590-4834; E-mail: weissmi@email.chop.edu.

[2] The abbreviations used are: Hb, hemoglobin; AHSP, α-hemoglobin-stabilizing protein; IRE, iron responsive element; IRP, iron regulatory protein; ROS, reactive oxygen species; TFR1, transferrin receptor 1; UTR, untranslated region; HRI, heme-regulated inhibitor kinase; FAC, ferric ammonium citrate; Hem, hemin; DFO, desferrioxamine; FTH1, ferritin heavy chain 1; HBA-A1, α-globin; mut, mutant; wt, wild-type; siRNA, small interfering RNAs; Δ*G*, free energy; Act-D, actinomycin-D; KD, knockdown; EMSA, electrophoretic mobility shift assay.

for example during iron deficiency, Bach 1 binds cis elements within α-globin, β-globin, and other genes to repress transcription (17). Binding of heme to Bach1 induces its release from DNA and proteolytic degradation, thereby promoting globin transcription (18, 19). Thus, Bach1 and HRI sense intracellular iron (via heme) and adjust globin synthesis appropriately to minimize the accumulation of free subunits.

α-Hemoglobin-stabilizing protein (AHSP) is an abundant erythroid protein that binds and stabilizes multiple forms of free α-globin (20, 21). For example, AHSP binds "apo" α-globin before heme insertion to stabilize folding of the nascent polypeptide (22). In addition, AHSP binds heme-associated "holo" α-globin (αHb) and converts it into a more stable form, which inhibits the ability of heme iron to catalyze ROS production (23, 24). In this fashion, AHSP may limit the toxicity of excess αHb that accumulates at low levels during normal erythropoiesis and to a greater extent in certain hemoglobinopathies, such as β-thalassemia. *Ahsp* gene knock-out mice produce short-lived erythrocytes with Hb precipitates, indicating an important role in normal erythropoiesis (25). In addition, loss of AHSP exacerbates β-thalassemia in mice, and quantitative variations in *AHSP* expression may influence the phenotypes of some forms of human β-thalassemia (25, 26).

Given the important functions of AHSP in normal erythropoiesis and its potential role as a quantitative trait modifier of β-thalassemia, it is important to define the mechanisms that govern *AHSP* gene expression. Previous studies demonstrated that the erythroid nuclear proteins GATA-1 and EKLF, and the more generalized factor Oct-1, positively regulate *AHSP* transcription (27–30). In the current study, we identified a predicted stem-loop structure in the 3′-UTR of *AHSP* mRNA. This structure resembles an IRE, although it deviates significantly from canonical sequences. In RNA gel shift experiments this IRE-like sequence binds IRPs poorly compared with the classical *FTH1* IRE. However, additional studies demonstrate that the *AHSP* mRNA stem-loop associates with IRPs in cells and modulates iron concentration-dependent mRNA stability. These findings extend the range of functional IRE-like structures that do not conform to previously defined IRE consensus sequences. In addition, they illustrate a new mechanism that links hemoglobin metabolism to cellular iron status.

EXPERIMENTAL PROCEDURES

Plasmids and Cloning Strategy—Full-length human AHSP cDNA was PCR-amplified using the following primer set: AHSP-Forward: 5′-ACAGAGAGATTCACGCACC-3′ and AHSP-Reverse1: 5′-CAACAAAACCAGCAGTGGTCTTTA-TTGAGG-3′. To generate the AHSP stem-loop mutant cDNA ($AHSP^{mut}$), a second reverse primer was used: AHSP-Reverse2: 5′- CAACAAAACCAGCAGTGGTACTCATTGAGG-3′. The three mutated nucleotides are underlined. PCR conditions were: 95 °C x 3 min; 94 °C × 30 s, 58 °C × 40 s, 72 °C × 1 min for 30 cycles; 72 °C × 4 min. Full-length cDNAs were cloned into pEF1-α^{NEO} or p-TET plasmids (Invitrogen). All wild-type (wt) and mutant AHSP cDNAs generated by PCR were sequenced.

Cell Lines and Culture Conditions—The K562 human erythroleukemia cell line was cultured in IMDM with 10% fetal bovine serum. HeLa/tTA cells (31) were cultured in Dulbecco's modified Eagle's medium with 10% fetal bovine serum. HeLa IRP knockdown (KD) cells were grown with puromycin and G418 (32). To induce erythroid maturation, K562 cells were treated with 80 μM hydroxyurea (Sigma) for 48 h. Cells were treated with either 1 mM ferric ammonium citrate (FAC) or 50 μM hemin (hem) as iron sources. Desferrioxamine (DFO, 100 μM) was used as an iron chelator. Cell transfection was performed with FuGENE (Roche Applied Sciences), according to the manufacturer's instructions. COS-7 and HeLa cells were transfected with 2 μg of $AHSP^{wt}$ pEF1-α^{NEO} or $AHSP^{mut}$ pEF1-α^{NEO} and analyzed after 48 h. HeLa/tTA cells, used for experiments in Fig. 2, were transfected with 2 μg of $AHSP^{wt}$ pTET or $AHSP^{mut}$ pTET and analyzed after 24 h. These experiments were performed in the absence of tetracycline to allow for full cDNA expression in this "tet-off" system.

Bioinformatics—We used RNAProfile to search for predicted stem-loops within AHSP mRNAs (33). Multispecies comparison of AHSP cDNAs was performed using The UCSC Genome Browser (34); the mouse and marmoset sequences were added by inspection. RNA secondary structures were evaluated further using RNAfold and mfold (35).

RNA Immunoprecipitation (IP)—Isolation of IRP-RNA complexes was performed as described with minor modifications (36). A detailed protocol is included in supplemental methods. Anti-IRP1 antibody was obtained from Santa Cruz Biotechnology. Anti-IRP2 antibody was provided by Tracey Rouault (37).

RNA-labeled Probe Synthesis—Radiolabeled IRE and control probes were prepared by *in vitro* transcription from oligonucleotide templates using T7 RNA polymerase (Invitrogen) (38). Templates consisted of a "bottom strand" oligomer containing the 17-nucleotide T7 RNA polymerase promoter sequence fused to IRE sequences. This was hybridized to a 17-nucleotide "top strand" that is complementary to the T7 promoter sequence represented in the bottom strand (supplemental Table S1). For competition assays, FPLC-purified RNA oligonucleotides were purchased from IDT (supplemental Table S1).

Electrophoretic Mobility Shift Assay (EMSA)—Purified IRPs were prepared as described (39, 40). [^{32}P]UTP-radiolabeled IRE probes (1 nM) were mixed with either 100 ng of liver cytoplasmic extract or different molar ratios of purified IRP1 or IRP2 and incubated for 10 min at room temperature. Heparin (3 mg/ml) was added, and the samples analyzed on a 6% native polyacrylamide gel as described (41).

Messenger RNA Stability Assay—Actinomycin D, 5 μM, (Sigma) was added to the culture medium to inhibit transcription. Cells were collect at various time points, washed with cold phosphate-buffered saline, and lysed with Trizol reagent (Invitrogen). The relative levels of *AHSP* and control mRNAs were determined by real time RT-PCR.

RNA Isolation and Gene Expression Analysis—Total RNA was purified by homogenizing cells in Trizol reagent (Invitrogen). Nuclear and cytoplasmic fractions of RNA were isolated as described (42). Ten million cells were incubated in 3 volumes of lysis buffer (10 mM Tris-HCl pH 7.4, 10 mM NaCl, 3 mM $MgCl_2$, 0.5% Nonidet P-40) for 5 min on ice. Nuclei were recovered by centrifugation (200 × *g* for 5 min). The supernatant was collected as cytoplasmic fraction. Nuclear pellets were washed twice with cold phosphate-buffered saline, and RNA was

extracted with Trizol reagent. RNA samples were treated with 1 unit of RNase-free DNase I (Invitrogen) for 20 min at 37 °C before cDNA synthesis.

Complementary DNA (cDNA) was generated using 2 μg of total RNA, oligo dT18, and SuperScript II reverse transcriptase (Invitrogen). Gene expression was quantified by real-time RT-PCR (Thermocycle 7900, Applied Biosystems) using SYBR green reagent (Invitrogen) and mRNA-specific primers (supplemental Table S2). Primers were designed for standard real-time PCR using PrimerExpress (Applied Biosystems).

RESULTS

Identification of a Putative Stem-Loop Structure in the 3′-UTR of AHSP mRNA—Iron regulates the expression of numerous genes via IRE stem-loop structures present in the UTRs of mRNA. We investigated whether *AHSP* mRNA might be subject to this mode of regulation by using the program RNAProfile to search for segments of the UTRs of human *AHSP* mRNA that have the potential to form stem-loops. A prominent potential stem-loop ($\Delta G = -9.50$ kcal/mol) is found at the 3′-end of the mRNA, with the polyadenylation signal as part of the predicted stem (Fig. 1). A similar predicted stem-loop structure is found in the homologous sequences of other simian primates, including the rhesus macaque, an Old World monkey, and marmoset, a New World monkey.

This stem-loop structure has several features in common with canonical IREs, including a 5-bp upper stem separated from a lower stem of variable length by an unpaired nucleotide in a bulge (43–45). The bulge can have a single unpaired nucleotide as in the IREs in the 3′-UTR of *TFR1* mRNA (Fig. 1*C*). The apical loop of most IREs has the consensus sequence CAGUGH (where H is A, C, or U), with the C forming a base pair with the second G to generate an AGU pseudotriloop structure that is recognized by IRP1 (46). The sequence of human *AHSP* mRNA has a matching sequence, CAGUGC. However, the predicted stem-loop structure for human *AHSP* mRNA differs in several aspects from canonical IREs. One predicted structure has the CA in the CAGUGC loop consensus motif involved in base pairing in the upper stem (Fig. 1*C*, *structure 1*). In an alternate conformation, the AGU is exposed and anchored by a G-C intraloop pair (*structure 2* in Fig. 1*C*), but this secondary structure is expected to be less stable. The preferred nucleotide in the bulge is C in all known natural IREs, whereas the predicted structures for *AHSP* mRNA have an A. The A nucleotide in the bulge is part of the AAUAAA polyadenylation signal.

Numerous studies have identified RNAs with non-canonical sequences that bind IRPs (44, 45, 47). In addition, several naturally occurring functional IREs that deviate from canonical criteria have been described (15, 48–53). We investigated further the functional properties of the IRE-like stem-loop element present in *AHSP* mRNA. We discovered that this stem-loop associates with IRE-binding proteins and modulates mRNA stability in an iron-dependent fashion. Therefore, we refer to this structure as an IRE-like stem-loop because it shares some properties with classical IREs but also exhibits significant differences in sequence, predicted secondary structure and some functional features.

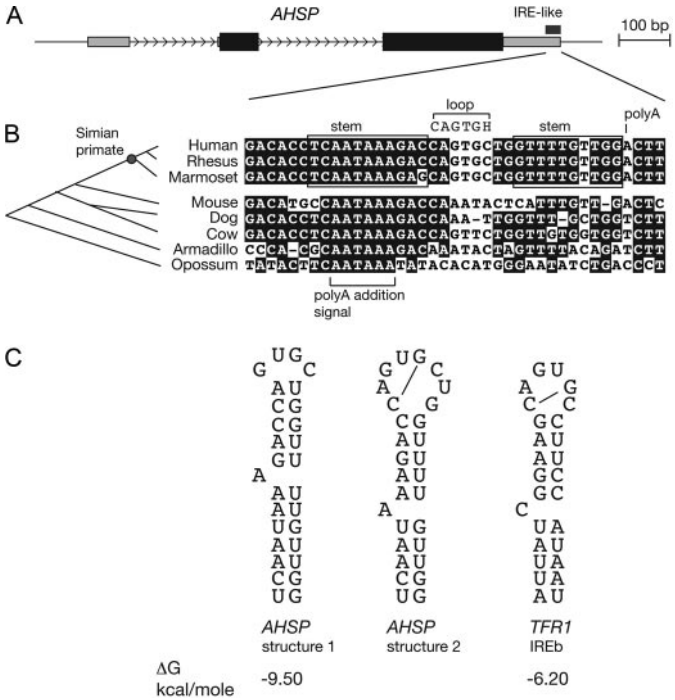

FIGURE 1. **Sequence, phylogenetic comparison and predicted structures of an IRE-like stem-loop in *AHSP* mRNA.** *A*, diagram of the human *AHSP* gene showing a 1100-bp interval of chr16:31,446,601–31,447,700 from the March 2006 assembly of the human genome. The 3 exons of the gene are shown as *boxes* with untranslated regions in *light gray* and protein-coding regions in *black*. The IRE-like stem-loop in the 3′-untranslated region is indicated as a *dark gray box* above the gene. *B*, multispecies alignment of sequences homologous to the region containing the human *AHSP* IRE-like stem-loop. *Shaded nucleotides* are found in at least 6 of the 8 species compared. Phylogenetic relationships are given in the tree to the *left* of the alignment. Nucleotides predicted to be in stems and loops in the IRE-like stem-loop of primate RNAs are indicated, along with the poly(A) addition signal and the poly(A) addition site. *C*, secondary structure predictions for the IRE-like stem-loop, along with the canonical structures for the human *TFR1* mRNA IRE. Within the loop, a *line* is drawn between the paired C-G in the CAGUG motif. The first *AHSP* structure gives the lowest predicted free energy (ΔG) by folding programs such as RNAfold. The second structure forces the AGU in the CAGUG motif to be unpaired, as is found in the structure of an IRE-IRP1 complex.

An *AHSP* IRE-like stem-loop is not apparent in mammals outside the clade of simian primates. As expected, the AAUAAA polyadenylation signal is conserved among all mammals including the marsupial opossum, but the sequences homologous to the apical loop and the 3′-part of the stem show many differences outside simian primates (Fig. 1*B*). Many of these sequences are predicted to form stem-loops, but they differ from those expected for IREs in the length of the stems, the presence of a bulge 5 bp away from the loop, and the sequence of the loop. Thus, the phylogenetic comparisons indicate that this IRE-like structure is primate-specific. It may be an adaptation in primates to provide an additional mechanism for iron-mediated regulation of *AHSP*.

The AHSP IRE-like Stem-Loop Associates with IRPs in Cells—We used RNA co-immunoprecipitation to study human *AHSP* mRNA binding to IRP1 and IRP2, the two major known IRE-binding proteins (54). We introduced a full-length wt *AHSP* cDNA expression construct into HeLa cells and immunoprecipitated IRP1 and IRP2 complexes from cytosolic extracts. Co-immunoprecipitated RNAs were quantified by real-time RT-

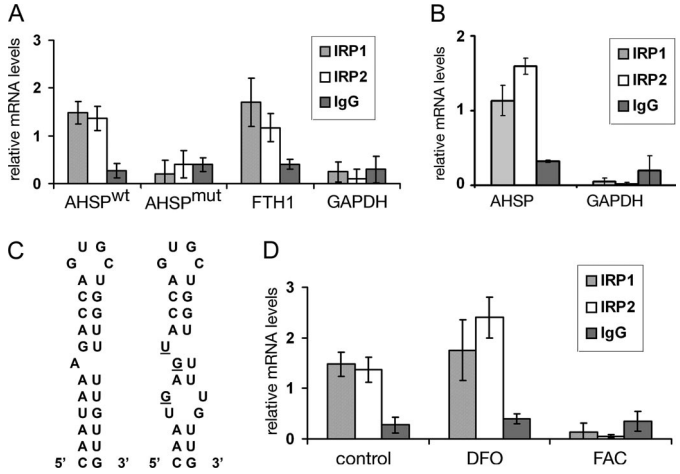

FIGURE 2. **Co-immunoprecipitation of *AHSP* mRNA with IRP1 and IRP2.** *A*, HeLa cells were transfected with plasmids encoding full-length human *AHSP* cDNA, either wt or a mutant (*mut*) forms containing three nucleotide substitutions that disrupt the stem-loop (*C*). Cytoplasmic extracts were incubated with specific antibodies for IRP1, IRP2, or control IgG. Antibody complexes were purified with protein G beads and the associated mRNAs quantified by real-time RT-PCR. The *y*-axis shows relative mRNA levels normalized to input (non-immunoprecipitated) RNA from each sample. Results are shown as mean values from three independent experiments with error bars indicating S.D. *B*, co-immunoprecipitation of IRPs and endogenous *AHSP* mRNA in K562 erythroleukemia cells, performed as described in *A*. *C*, stem-loop structures of AHSP IRE^{wt} (*left*) and AHSP IRE^{mut} (*right*) with nucleotide changes *underlined*. *D*, the effects of DFO or FAC on IRP binding to *AHSP*^{wt} mRNA in HeLa cells, performed as described in *A*.

PCR and normalized to the same mRNA present in extracts prior to immunoprecipitation (input sample). Ectopically expressed *AHSP*^{wt} mRNA was enriched significantly by immunoprecipitation with IRP1 or IRP2 antibodies, but not control IgG (Fig. 2*A*). Identical results were obtained using two independent sets of PCR primers derived from different regions of *AHSP* cDNA (data not shown). *FTH1* mRNA examined as a positive control also co-immunoprecipitated specifically with IRP1 and IRP2 (Fig. 2*A*). Glyceraldehyde phosphate dehydrogenase (*GAPDH*) mRNA, which does not contain an IRE, was not enriched by IRP immunoprecipitation (Fig. 2*A*). Endogenous *AHSP* mRNA was also enriched in IRP1 and IRP2 complexes immunoprecipitated from cytosolic extracts of K562 erythroleukemia cells (Fig. 2*B*). Together, these data suggest that *AHSP* mRNA associates with IRP1 and IRP2 in cells.

To determine if the *AHSP* mRNA-IRP interaction is mediated by the IRE-like stem-loop, we generated *AHSP*^{mut} cDNA, which contains three mutations that disrupt the structure (Fig. 2*C*). This mutant cDNA was expressed normally in HeLa cells (not shown), but failed to bind IRPs 1 and 2 (Fig. 2*A*). Hence, *AHSP* mRNA associates with IRPs 1 and 2 via the IRE-like stem-loop present in the 3′-UTR. We also investigated the effects of iron on *AHSP* mRNA binding affinity to IRPs. IRP1 and IRP2 complexes were immunoprecipitated from *AHSP*^{wt} mRNA-expressing HeLa cells treated with either ferric ammonium citrate (FAC) as a source of iron or desferrioxamine (DFO), an iron chelator (Fig. 2*D*). Treatment with DFO moderately enhanced co-immunoprecipitation between IRP2 and *AHSP* mRNA ($p < 0.05$). In contrast, FAC treatment markedly inhibited co-immunoprecipitation of *AHSP* mRNA with both IRPs 1 and 2 (Fig. 2*D*), without impairing cell viability (not shown). Overall, our data indicate that in cells, the *AHSP* mRNA IRE-like stem-loop associates with IRPs in an iron-regulated fashion, consistent with classical IRE/IRP interactions described for other transcripts, including *FTH1*, *TFR1*, and *ALAS2* (46, 55, 56).

The AHSP IRE-like Stem-Loop Binds Poorly to IRPs in Vitro—We performed RNA EMSAs to further study *AHSP* IRE-like stem-loop-IRP interactions (Fig. 3). A [^{32}P]UTP-labeled RNA oligonucleotide representing the IRE-like structure from human *AHSP* mRNA was incubated with several concentrations of purified IRP1 and IRP2 and RNA-protein interactions examined by non-denaturing polyacrylamide electrophoresis (Fig. 3*A*). Human *FTH1* IRE probe was used as a positive control for binding to IRPs. Upon incubation with the *FTH1* IRE probe (1 nM), both recombinant IRP1 (1 nM) and IRP2 (1 nM) showed prominent band-shifts, indicating the formation of RNA:protein complexes (Fig. 3*A*, *lanes 1* and *2*). In contrast, the *AHSP* IRE-like stem-loop probe exhibited very weak IRP binding activity. Formation of RNA-IRP1 complex was visualized only at RNA/protein ratios of 1:5 and 1:10 (Fig. 3*A*, *lanes 4–6*). No band shift was visualized at any concentration of IRP2 (Fig. 3*A*, *lanes 7–9*). Next, we performed gel shift competition assays. Liver cell extracts (as a source for IRP1 and IRP2) were incubated with [^{32}P]UTP-labeled *FTH1* IRE probe and various unlabeled competitor RNAs, then formation of RNA-protein complexes was evaluated by EMSA (Fig. 3*B*). At 5-fold competitor excess, unlabeled *FTH1* IRE probe efficiently competed with labeled probe, disrupting most of the [^{32}P]RNA-protein complex (Fig. 3*B*, *lane 2* and *C*). In contrast, higher concentrations of the unlabeled *AHSP* probe were required for competition with the *FTH1* IRE (Fig. 3*B*, *lanes 6–9* and *C*). The reduced *FTH1* probe complexes resulting from addition of 30–50-fold excess cold *AHSP* probe (*lanes 8* and *9*) appear to represent specific but relatively low affinity binding of the latter to IRPs, because the same concentrations of a control scrambled unlabeled probe had no effect (Fig. 3*B*, *lanes 12–13* and *C*).

In summary, radiolabeled *AHSP* IRE-like stem-loop probe binds purified IRP1 only weakly and no binding to IRP2 was detected in EMSA experiments. This is consistent with findings that *in vitro* binding of IRP2 to IRE stem-loops exhibits more stringent requirements for nucleotide sequences in the bulge region (57). These EMSA results contrast with our findings that both IRP1 and IRP2 specifically co-immunoprecipitate with *AHSP* mRNA in cell extracts (see "Discussion").

Iron Destabilizes Endogenous AHSP mRNA in Erythroleukemia Cells—We next sought to investigate functional properties of the AHSP IRE-like stem-loop. Binding of IRPs to 3′-UTR IREs increases mRNA stability by protecting against endonucleolytic cleavage (13). The most studied example is *TFR1* mRNA, which contains multiple IREs in the 3′-UTR (13, 58–62). Under iron-deficient conditions, IRPs bind to *TFR1* transcripts and increase their half-life. In contrast, high levels of iron cause release of IRPs, promoting mRNA degradation. We examined the effects of iron on the stability of endogenous *AHSP* mRNA transcripts in K562 erythroleukemia cells (Fig. 4*A*). Cells were treated for 16 h with FAC as an iron source or DFO to deplete iron. Actinomycin-D was added to arrest transcription and the kinetics of mRNA decay was measured by

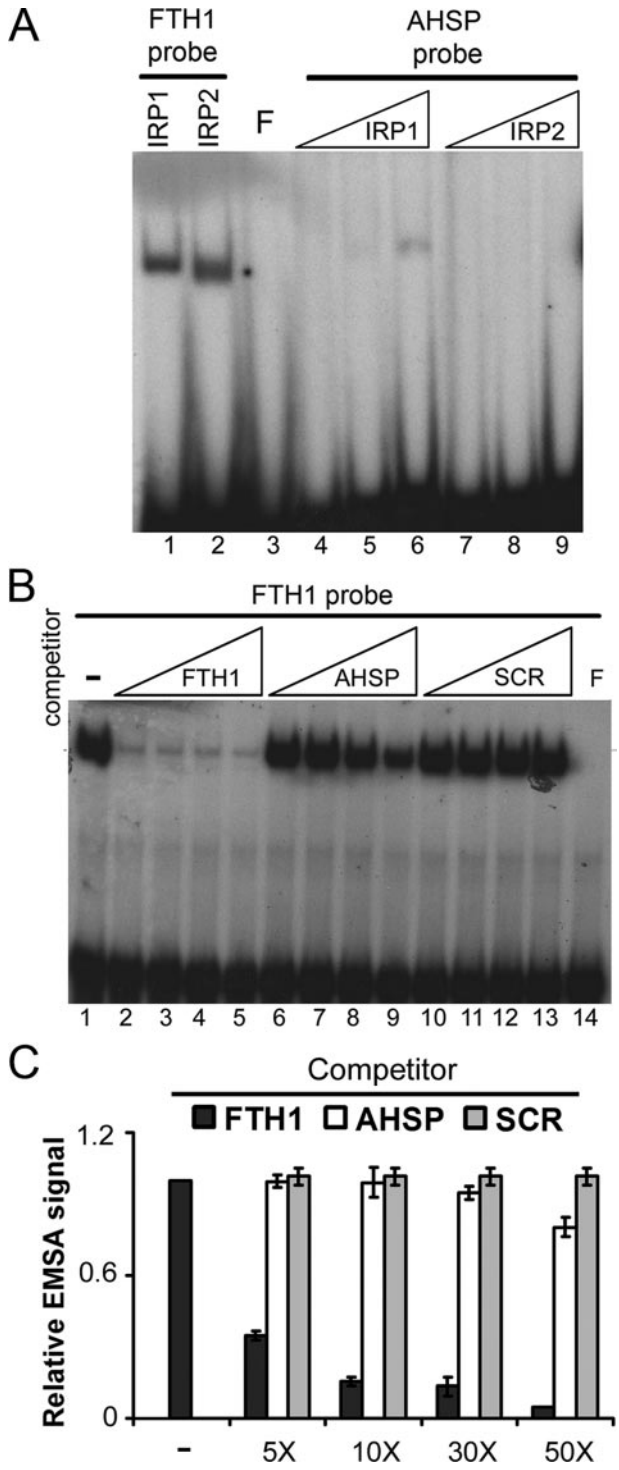

FIGURE 3. **EMSA analysis of *AHSP* mRNA stem-loop-IRP interactions.** *A*, radiolabeled RNA probes encoding *FTH1* or *AHSP* IRE stem-loops (1 nM) were incubated with increasing amounts of recombinant IRP1 or IRP2 (1, 5, and 10 nM). Protein-mRNA complexes were fractionated by polyacrylamide gel electrophoresis and detected by autoradiography. *B*, labeled *in vitro* transcribed *FTH1* IRE probe (1 nM) was incubated with liver cell cytoplasmic extract (100 ng) and increasing concentrations of cold competitor RNAs encoding the *FTH1* IRE, the human *AHSP* IRE-like stem-loop or scrambled oligoribonucleotide (5×, 10×, 30×, or 50× excess compared with labeled probe). *F* stands for free probe-only reaction. *C*, EMSA signals for IRP-RNA complexes shown in *B* were quantified by phosphorimage analysis and plotted as shown. The EMSA signal obtained in the absence of competitor (−) is designated as 1.0. The fraction of this signal remaining after incubation with various competitors is indicated. Results are shown as mean values from three independent EMSA experiments with error bars indicating S.D.

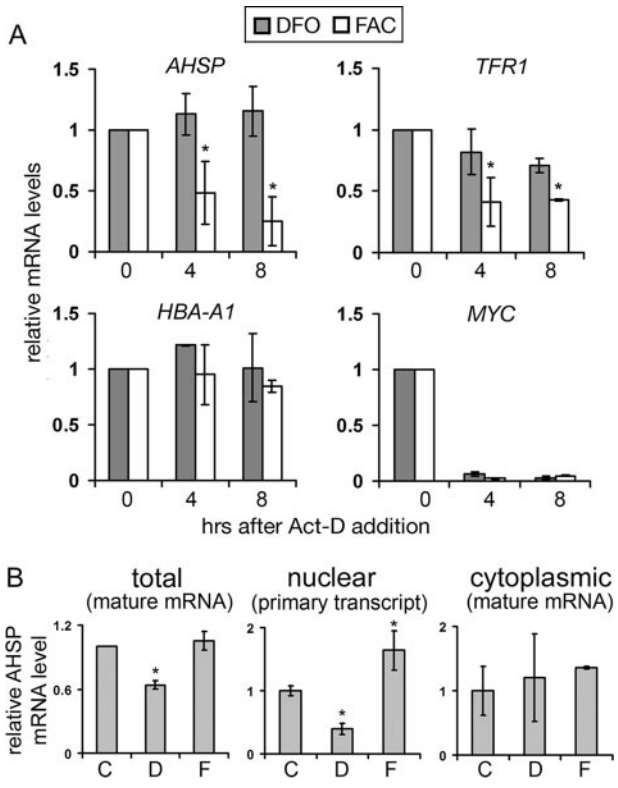

FIGURE 4. **Effects of iron on endogenous *AHSP* mRNA in K562 erythroleukemia cells.** *A*, iron destabilizes *AHSP* mRNA. K562 cells were treated with the iron chelator DFO or FAC for 16 h, then actinomycin-D (*Act-D*), 5 μM, was added to arrest transcription. *AHSP* and control mRNAs were quantified by real-time RT-PCR at the indicated timepoints. The *y*-axis shows relative mRNA levels with time 0 designated as 1.0. Each mRNA sample was normalized to *GAPDH* mRNA. Control mRNAs include transferrin receptor (*TFR1*), which is destabilized by iron, α-*globin* (*HBA-A1*), a stable, non iron-regulated mRNA, and *MYC*, a constitutively unstable mRNA. Results are shown as mean values from three independent experiments with error bars indicating S.D. *, $p <$ 0.05 for FAC-treated samples at $t = 0$ *versus* 4 and 8 h, Student's *t* test. *B*, effects of iron on steady-state *AHSP* mRNA. K562 cells were treated with DFO (*D*) or FAC (*F*) for 16 h, and *AHSP* RNA was quantified in whole cell extracts, nucleus, and cytoplasm. Mature mRNA was measured in the cytoplasm and in whole cells. *AHSP* mRNA primary transcripts were measured in nuclear fractions using primers surrounding exon 2 and intron 2. Results are shown as mean values from three independent experiments with error bars indicating S.D. *, $p < 0.05$ *versus* control sample.

real-time RT-PCR. Transcript levels were normalized to those of *GAPDH*. As internal controls, α-*globin* (*HBA-A1*) and *MYC* mRNAs were examined as examples of constitutively stable and unstable transcripts, respectively (63). In K562 cells treated with DFO, *AHSP* mRNA was relatively stable, with a half-life greater than 8 h (Fig. 4*A*, *upper left panel*). In contrast, *AHSP* mRNA was more rapidly degraded with a half-life of ~4 h in FAC-treated cells. As expected, endogenous *TFR1* mRNA was destabilized by iron (13, 60). In addition, *HBA-A1* and *MYC* RNAs which do not contain IREs were unaffected by either drug. Thus, endogenous *AHSP* mRNA is destabilized by iron in human hematopoietic cells, consistent with the presence of a functional 3′-UTR IRE.

Somewhat surprisingly, DFO treatment of K562 cells decreased the steady state level of mature *AHSP* mRNA measured in whole cell extracts by ~30% (Fig. 4*B*, *first panel*), despite concurrent mRNA stabilization, as shown in Fig. 4*A*. To reconcile these findings, we examined *AHSP* mRNA in nuclear and cytoplasmic fractions of DFO- and FAC-treated cells. In the

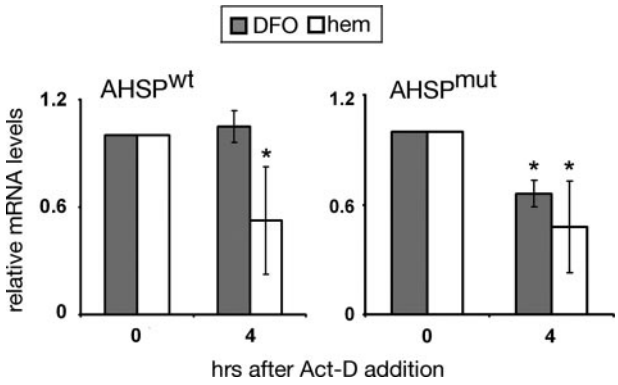

FIGURE 5. **The *AHSP* 3′-UTR stem-loop confers iron-regulated mRNA stability.** COS-7 cells were transfected with plasmids encoding full-length human *AHSP* cDNA, either wt or the stem-loop-mutated form (*mut*). Cells were treated for 16 h with hemin (*hem*), as a source of iron or DFO, and mRNA stability was measured after addition of actinomycin-D, as described in the legend to Fig. 4. Results are shown as mean values from three independent experiments with error bars indicating S.D. *, $p < 0.05$ for $t = 0$ *versus* 4 h, Student's *t* test.

nucleus, FAC treatment increased the level of *AHSP* primary transcripts, while DFO treatment produced an opposite effect (Fig. 4*B*, *second panel*). Together these results indicate that in K562 cells, iron increases *AHSP* gene transcription or nuclear RNA stability and concurrently destabilizes the mature mRNA. The net effect is little change in mature cytoplasmic mRNA (Fig. 4*B*, *third panel*). Hence, iron has multiple opposing effects on *AHSP* gene expression in K562 cells. *In vivo*, the relative importance of each individual effect during erythropoiesis is likely dependent on developmental stage and cellular milieu (see "Discussion").

The AHSP IRE-like Stem-Loop Mediates Iron-regulated mRNA Stability—The previous experiment demonstrated that iron levels modulate *AHSP* mRNA stability. To test whether this mode of regulation occurs via the 3′-UTR IRE-like structure, we measured the effects of iron on $AHSP^{mut}$ RNA, in which the stem-loop sequence is mutated to impair IRP binding (Fig. 2, *A* and *C*). We expressed $AHSP^{wt}$ and $AHSP^{mut}$ mRNAs in COS cells treated with hemin (hem) as a source of iron or DFO and measured the rate of transcript decay after transcriptional arrest induced by actinomycin-D (Fig. 5). Similar to what we observed for endogenous transcripts in hematopoietic cells (Fig. 4, *above*), $AHSP^{wt}$ mRNA was stable under low-iron conditions and degradation was accelerated by iron. In contrast, the mutant mRNA was constitutively unstable, independent of added iron. The most likely explanation for these findings is that when the IRE structure is disrupted, IRPs can no longer bind the 3′-UTR of $AHSP^{mut}$ mRNA. This renders the transcript more susceptible to endonucleolytic cleavage, even when iron concentrations are low. Thus, the effects of iron on *AHSP* mRNA stability maps to its IRE-like stem-loop.

AHSP mRNA Stability Is Directly Regulated by IRPs—To further study the role of IRPs in regulating *AHSP* mRNA stability, we used HeLa cell lines that stably express small interfering RNAs (siRNAs) against IRP1 (IRP1 KD), IRP2 (IRP2 KD), or both (IRP1/2 KD)(32). We expressed *AHSP* mRNA in wt and IRP KD cells and measured transcript levels before and 8 h after actinomycin-D treatment (Fig. 6). After blocking transcription

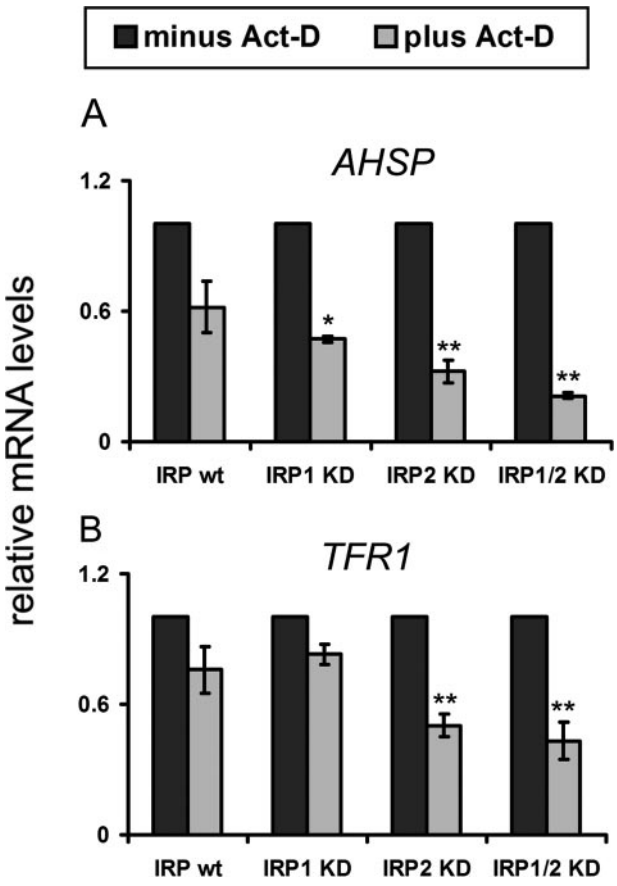

FIGURE 6. **Deficiency of IRP1 or IRP2 destabilizes *AHSP* mRNA.** *A*, wt HeLa cells and KD lines expressing siRNAs targeting IRP1, IRP2, or both were transfected with a full-length human *AHSP* cDNA expression plasmid and mRNA stability was measured 8 h after addition of actinomycin-D, as described in the legend to Fig. 4. Results are shown as mean values from three independent experiments with error bars indicating S.D. *, $p = 0.16$; **, $p < 0.05$ (*versus* wt sample treated with Act-D), Student's *t* test.

AHSP mRNA was reduced by ~40% in wt cells. In contrast, loss of IRP1 or IRP2 decreased *AHSP* mRNA by ~50 and 70%, respectively (Fig. 6*A*). The effects of IRP reduction were additive, as *AHSP* mRNA was reduced by about 80% in IRP 1/2 KD cells. Hence, both IRP1 and IRP2 can stabilize *AHSP* mRNA in cells.

Three controls show that this experimental approach replicates important aspects of IRE regulation. First, endogenous *TFR1* mRNA was preferentially destabilized in IRP2 KD and IRP1/2 KD cells, as previously reported (32) (Fig. 6*B*). Second, *FTH1* mRNA levels were not affected by lack of IRPs, because IRPs regulate translation but not stability of this mRNA (64) (data not shown). Third, *MYC* mRNA levels rapidly declined after actinomycin-D treatment in either cell line, consistent with IRP-independent instability of this transcript (data not shown). Together, these results demonstrate that *AHSP* mRNA stability is regulated by iron-dependent interactions between IRP1 and IRP2 and a non-canonical 3′-UTR IRE-like stem loop.

DISCUSSION

Until recently, IREs were believed to be associated with relatively strict consensus sequences present in a few genes that are

directly involved in iron metabolism, such as *ALAS2*, *TFR*, and *FTH1* (46, 55, 56). However, several lines of study indicate that IREs and related elements are more diverse in structure and distribution. Unbiased *in vitro* selection methods show that non-canonical IRE sequences form stem-loops that can bind IRPs (44, 47). In addition, numerous mRNAs contain IREs that deviate significantly from consensus sequences (15, 48, 50–53). The crystal structure of an IRP1-*FTH1* IRE complex indicates how IRPs may recognize different sets of IRE sequences through alternate subsets of bonding amino acids (46). The 3′-UTR of *AHSP* mRNA contains an IRE-like stem-loop that deviates from consensus and recognizes IRPs poorly *in vitro*, yet associates with IRP1 and IRP2 *in vivo* to regulate *AHSP* mRNA stability according to iron concentration. These data show that IRPs can regulate mRNA expression through non-canonical IREs.

In cell extracts, co-immunoprecipitation of IRP1 and IRP2 with *AHSP* mRNA is mediated by an IRE-like stem-loop structure. However, in EMSA, a short (32 bp) oligoribonucleotide probe containing this IRE-like element bound poorly to IRP1 and no binding to IRP2 was detected. Several features of the *AHSP* IRE-like stem-loop are predicted to impair its interactions with IRPs. These include the shifted position of the CAGUGH loop consensus sequence and the presence of A at the stem bulge (see Fig. 1) (45, 46). It is possible that additional factors not present in the EMSA reactions strengthen the binding of IRPs to the *AHSP* IRE-like stem-loop *in vivo*. For example, extended sequences in the *AHSP* mRNA that were not present in the EMSA probe may optimize folding of an IRE-like structure (41). In addition, accessory cellular proteins absent in purified IRP preparations may enhance *AHSP* IRE-like stem-loop:IRP interactions. It is also possible that IRPs associate with the *AHSP* IRE-like stem-loop indirectly as part of higher order protein complexes. This may be true in particular for IRP2, where EMSA failed to detect any interaction with the *AHSP* IRE-like stem-loop, despite our observations that *AHSP* mRNA co-immunoprecipitates with IRP2 in cell extracts and that the message is destabilized by IRP2 knockdown. Regardless of the underlying mechanisms, the RNA immunoprecipitation assay may provide a more sensitive context for detecting biologically relevant IRP associations with atypical IREs. One important general implication of our findings is that IRE-like stem-loop structures that bind IRPs weakly (or not at all) *in vitro* can still associate with IRPs in cells to regulate mRNA expression.

It is interesting to consider the *AHSP* IRE-like structure in context of the general evolution of the IRE regulatory module (65). Some IREs, such as those present in ferritin genes and *TRF1*, occur in most metazoan species. Others, such as those found in the divalent metal transporter 1 (*DMT1*) gene, are largely restricted to mammals. The IRE-like stem-loop involved in modulating the response of *AHSP* to iron has an even more restricted phylogenetic distribution. It is only found in simian primates and thus appears to be an adaptation in this lineage. If so, the primate IRE-like element was generated from sequences that include a polyadenylation signal. Thus, these sequences in primates are under constraint for two functions and that may account for some of the non-canonical features of this IRE-like element. For example, it is possible that the constraint to maintain an AAUAAA polyadenylation signal outweighs the constraint for a C in the bulge in the stem-loop of the IRE-like structure.

The *AHSP* gene has been identified to date only in mammals, including eutherians and marsupials. No evidence for a homolog to *AHSP* has been observed in other tetrapods such as chickens, lizards or amphibians. This suggests that the AHSP protein has appeared relatively recently in evolution as a mechanism to fine-tune hemoglobin synthesis and homeostasis (66). Acquisition of the IRE-like structure in primates may represent a new level of control through which the stability of a hemoglobin subunit is modulated according to iron concentration within developing erythroid cells.

Iron destabilized endogenous *AHSP* mRNA in K562 human erythroleukemia cells, most likely by causing release of IRPs from the IRE-like structure in the 3′-UTR. However, iron simultaneously increased levels of nascent primary transcripts (Fig. 5). Our preliminary unpublished data indicate that the transcriptional repressor Bach1 binds the *AHSP* gene (MJW and COS). Thus, iron may activate transcription by inducing the synthesis of heme, which binds Bach1 causing its release from DNA and replacement by a positively acting transcription factor (17). These opposing effects reflect multilayered mechanisms of gene regulation for *AHSP* and are consistent with findings that the effects of iron on expression of IRE-regulated genes vary according to cell type and developmental stage (15, 67). *In vivo*, the net effects of IRP interactions with the *AHSP* mRNA IRE-like structure may predominate during later stages of erythropoiesis as transcription subsides.

Several biological implications for the *AHSP* IRE-like stem-loop are possible based on known functions of the protein. For example, in iron deficiency apo globins accumulate due to reduced heme synthesis. Apo α-globin is particularly unstable, as evidenced by its reduced secondary structure in solution (68). Moreover, α-globin precipitation is relatively increased in iron deficiency (69). AHSP binds newly synthesized apo α-globin to enhance its folding and solubility (22). Induction of AHSP production via IRP interactions at the 3′-UTR may provide a compensatory mechanism to stabilize excess apo α-globin during iron deficiency. Another function of AHSP is to bind and detoxify excess free αHb, which is present at high levels in β-thalassemia (24, 25). This disorder is frequently accompanied by iron overload from increased dietary absorption and red blood cell transfusions. Free iron causes tissue damage by catalyzing the production of ROS. In addition, the current study indicates that iron overload promotes degradation of *AHSP* mRNA by reducing IRP/IRE interactions. In this case, consequent reduction of AHSP protein could further destabilize accumulated αHb, enhancing its toxicity in erythroid cells of individuals with β-thalassemia.

Acknowledgments—We thank Stephen Liebhaber, Tracey Rouault, and Suzy and Frank Torti for advice and reagents.

REFERENCES

1. Beutler, E., Hoffbrand, A. V., and Cook, J. D. (2003) *Hematology Am. Soc. Hematol. Educ. Program*, 40–61
2. Rouault, T. A. (2006) *Nat. Chem. Biol.* **2,** 406–414
3. Muckenthaler, M. U., Galy, B., and Hentze, M. W. (2008) *Annu. Rev. Nutr.* **28,** 197–213
4. Wallander, M. L., Leibold, E. A., and Eisenstein, R. S. (2006) *Biochim. Biophys. Acta* **1763,** 668–689
5. Haile, D. J., Rouault, T. A., Harford, J. B., Kennedy, M. C., Blondin, G. A., Beinert, H., and Klausner, R. D. (1992) *Proc. Natl. Acad. Sci. U. S. A.* **89,** 11735–11739
6. Guo, B., Yu, Y., and Leibold, E. A. (1994) *J. Biol. Chem.* **269,** 24252–24260
7. Iwai, K., Klausner, R. D., and Rouault, T. A. (1995) *EMBO J.* **14,** 5350–5357
8. Goessling, L. S., Mascotti, D. P., and Thach, R. E. (1998) *J. Biol. Chem.* **273,** 12555–12557
9. Ishikawa, H., Kato, M., Hori, H., Ishimori, K., Kirisako, T., Tokunaga, F., and Iwai, K. (2005) *Mol. Cell* **19,** 171–181
10. Jeong, J., Rouault, T. A., and Levine, R. L. (2004) *J. Biol. Chem.* **279,** 45450–45454
11. Haile, D. J., Hentze, M. W., Rouault, T. A., Harford, J. B., and Klausner, R. D. (1989) *Mol. Cell Biol.* **9,** 5055–5061
12. Casey, J. L., Hentze, M. W., Koeller, D. M., Caughman, S. W., Rouault, T. A., Klausner, R. D., and Harford, J. B. (1988) *Science* **240,** 924–928
13. Mullner, E. W., and Kuhn, L. C. (1988) *Cell* **53,** 815–825
14. Gunshin, H., Allerson, C. R., Polycarpou-Schwarz, M., Rofts, A., Rogers, J. T., Kishi, F., Hentze, M. W., Rouault, T. A., Andrews, N. C., and Hediger, M. A. (2001) *FEBS Lett.* **509,** 309–316
15. Sanchez, M., Galy, B., Dandekar, T., Bengert, P., Vainshtein, Y., Stolte, J., Muckenthaler, M. U., and Hentze, M. W. (2006) *J. Biol. Chem.* **281,** 22865–22874
16. Chen, J. J. (2007) *Blood* **109,** 2693–2699
17. Igarashi, K., and Sun, J. (2006) *Antioxid. Redox. Signal* **8,** 107–118
18. Tahara, T., Sun, J., Igarashi, K., and Taketani, S. (2004) *Biochem. Biophys. Res. Commun.* **324,** 77–85
19. Tahara, T., Sun, J., Nakanishi, K., Yamamoto, M., Mori, H., Saito, T., Fujita, H., Igarashi, K., and Taketani, S. (2004) *J. Biol. Chem.* **279,** 5480–5487
20. Gell, D., Kong, Y., Eaton, S. A., Weiss, M. J., and Mackay, J. P. (2002) *J. Biol. Chem.* **277,** 40602–40609
21. Kihm, A. J., Kong, Y., Hong, W., Russell, J. E., Rouda, S., Adachi, K., Simon, M. C., Blobel, G. A., and Weiss, M. J. (2002) *Nature* **417,** 758–763
22. Yu, X., Kong, Y., Dore, L. C., Abdulmalik, O., Katein, A. M., Zhou, S., Choi, J. K., Gell, D., Mackay, J. P., Gow, A. J., and Weiss, M. J. (2007) *J. Clin. Investig.* **117,** 1856–1865
23. Feng, L., Gell, D. A., Zhou, S., Gu, L., Kong, Y., Li, J., Hu, M., Yan, N., Lee, C., Rich, A. M., Armstrong, R. S., Lay, P. A., Gow, A. J., Weiss, M. J., Mackay, J. P., and Shi, Y. (2004) *Cell* **119,** 629–640
24. Feng, L., Zhou, S., Gu, L., Gell, D. A., Mackay, J. P., Weiss, M. J., Gow, A. J., and Shi, Y. (2005) *Nature* **435,** 697–701
25. Kong, Y., Zhou, S., Kihm, A. J., Katein, A. M., Yu, X., Gell, D. A., Mackay, J. P., Adachi, K., Foster-Brown, L., Louden, C. S., Gow, A. J., and Weiss, M. J. (2004) *J. Clin. Investig.* **114,** 1457–1466
26. Lai, M. I., Jiang, J., Silver, N., Best, S., Menzel, S., Mijovic, A., Colella, S., Ragoussis, J., Garner, C., Weiss, M. J., and Thein, S. L. (2006) *Br. J. Haematol.* **133,** 675–682
27. Pilon, A. M., Nilson, D. G., Zhou, D., Sangerman, J., Townes, T. M., Bodine, D. M., and Gallagher, P. G. (2006) *Mol. Cell Biol.* **26,** 4368–4377
28. Gallagher, P. G., Liem, R. I., Wong, E., Weiss, M. J., and Bodine, D. M. (2005) *J. Biol. Chem.* **280,** 39016–39023
29. Keys, J. R., Tallack, M. R., Hodge, D. J., Cridland, S. O., David, R., and Perkins, A. C. (2007) *Br. J. Haematol.* **136,** 150–157
30. Hodge, D., Coghill, E., Keys, J., Maguire, T., Hartmann, B., McDowall, A., Weiss, M., Grimmond, S., and Perkins, A. (2006) *Blood* **107,** 3359–3370
31. Kong, J., Ji, X., and Liebhaber, S. A. (2003) *Mol. Cell Biol.* **23,** 1125–1134
32. Wang, W., Di, X., D'Agostino, R. B., Jr., Torti, S. V., and Torti, F. M. (2007) *J. Biol. Chem.* **282,** 24650–24659
33. Pavesi, G., Mauri, G., Stefani, M., and Pesole, G. (2004) *Nucleic Acid Res.* **32,** 3258–3269
34. Miller, W., Rosenbloom, K., Hardison, R. C., Hou, M., Taylor, J., Raney, B., Burhans, R., King, D. C., Baertsch, R., Blankenberg, D., Kosakovsky Pond, S. L., Nekrutenko, A., Giardine, B., Harris, R. S., Tyekucheva, S., Diekhans, M., Pringle, T. H., Murphy, W. J., Lesk, A., Weinstock, G. M., Lindblad-Toh, K., Gibbs, R. A., Lander, E. S., Siepel, A., Haussler, D., and Kent, W. J. (2007) *Genome Res.* **17,** 1797–1808
35. Zuker, M., and Stiegler, P. (1981) *Nucleic Acids Res.* **9,** 133–148
36. Waggoner, S. A., and Liebhaber, S. A. (2003) *Mol. Cell Biol.* **23,** 7055–7067
37. Meyron-Holtz, E. G., Ghosh, M. C., Iwai, K., LaVaute, T., Brazzolotto, X., Berger, U. V., Land, W., Ollivierre-Wilson, H., Grinberg, A., Love, P., and Rouault, T. A. (2004) *EMBO J.* **23,** 386–395
38. Allerson, C. R., Cazzola, M., and Rouault, T. A. (1999) *J. Biol. Chem.* **274,** 26439–26447
39. Brown, N. M., Anderson, S. A., Steffen, D. W., Carpenter, T. B., Kennedy, M. C., Walden, W. E., and Eisenstein, R. S. (1998) *Proc. Natl. Acad. Sci. U. S. A.* **95,** 15235–15240
40. Iwai, K., Drake, S. K., Wehr, N. B., Weissman, A. M., LaVaute, T., Minato, N., Klausner, R. D., Levine, R. L., and Rouault, T. A. (1998) *Proc. Natl. Acad. Sci. U. S. A.* **95,** 4924–4928
41. Barton, H. A., Eisenstein, R. S., Bomford, A., and Munro, H. N. (1990) *J. Biol. Chem.* **265,** 7000–7008
42. Feng, Y. Q., Warin, R., Li, T., Olivier, E., Besse, A., Lobell, A., Fu, H., Lin, C. M., Aladjem, M. I., and Bouhassira, E. E. (2005) *Mol. Cell Biol.* **25,** 3864–3874
43. Henderson, B. R., Menotti, E., Bonnard, C., and Kuhn, L. C. (1994) *J. Biol. Chem.* **269,** 17481–17489
44. Butt, J., Kim, H. Y., Basilion, J. P., Cohen, S., Iwai, K., Philpott, C. C., Altschul, S., Klausner, R. D., and Rouault, T. A. (1996) *Proc. Natl. Acad. Sci. U. S. A.* **93,** 4345–4349
45. Meehan, H. A., and Connell, G. J. (2001) *J. Biol. Chem.* **276,** 14791–14796
46. Walden, W. E., Selezneva, A. I., Dupuy, J., Volbeda, A., Fontecilla-Camps, J. C., Theil, E. C., and Volz, K. (2006) *Science* **314,** 1903–1908
47. Sierzputowska-Gracz, H., McKenzie, R. A., and Theil, E. C. (1995) *Nucleic Acid Res.* **23,** 146–153
48. Sanchez, M., Galy, B., Muckenthaler, M. U., and Hentze, M. W. (2007) *Nat. Struct. Mol. Biol.* **14,** 420–426
49. Huang, T.-S., Melefors, O., Lind, M. I., and Soderhall, K. (1999) *Insect Biochem. Mol. Biol.* **29,** 1–9
50. Friedlich, A. L., Tanzi, R. E., and Rogers, J. T. (2007) *Mol. Psychiatry* **12,** 222–223
51. Solano-Gonzalez, E., Burrola-Barraza, E., Leon-Sicairos, C., Avila-Gonzalez, L., Gutierrez-Escolano, L., Ortega-Lopez, J., and Arroyo, R. (2007) *FEBS Lett.* **581,** 2919–2928
52. Rogers, J. T., Randall, J. D., Cahill, C. M., Eder, P. S., Huang, X., Gunshin, H., Leiter, L., McPhee, J., Sarang, S. S., Utsuki, T., Greig, N. H., Lahiri, D. K., Tanzi, R. E., Bush, A. I., Giordano, T., and Gullans, S. R. (2002) *J. Biol. Chem.* **277,** 45518–45528
53. Cmejla, R., Petrak, J., and Cmejlova, J. (2006) *Biochem. Biophys. Res. Commun.* **341,** 158–166
54. Sanchez, M., Galy, B., Hentze, M. W., and Muckenthaler, M. U. (2007) *Nat. Protoc.* **2,** 2033–2042
55. Schlegl, J., Gegout, V., Schlager, B., Hentze, M. W., Westhof, E., Ehresmann, C., Ehresmann, B., and Romby, P. (1997) *Rna* **3,** 1159–1172
56. Dandekar, T., Stripecke, R., Gray, N. K., Goossen, B., Constable, A., Johansson, H. E., and Hentze, M. W. (1991) *EMBO J.* **10,** 1903–1909
57. Ke, Y., Sierzputowska-Gracz, H., Gdaniec, Z., and Theil, E. C. (2000) *Biochemistry* **39,** 6235–6242
58. Koeller, D. M., Casey, J. L., Hentze, M. W., Gerhardt, E. M., Chan, L.-N. L., Klausner, R. D., and Harford, J. B. (1989) *Proc. Natl. Acad. Sci. U. S. A.* **86,** 3574–3578
59. Rouault, T., Rao, K., Harford, J., Mattia, E., and Klausner, R. D. (1985) *J. Biol. Chem.* **260,** 14862–14866
60. Seiser, C., Posch, M., Thompson, N., and Kuhn, L. C. (1995) *J. Biol. Chem.* **270,** 29400–29406
61. Erlitzki, R., Long, J. C., and Theil, E. C. (2002) *J. Biol. Chem.* **277,** 42579–42587
62. Binder, R., Horowitz, J. A., Basilion, J. P., Koeller, D. M., Klausner, R. D.,

and Harford, J. B. (1994) *EMBO J.* **13,** 1969–1980
63. Rodgers, N. D., Wang, Z., and Kiledjian, M. (2002) *Rna* **8,** 1526–1537
64. Caughman, S. W., Hentze, M. W., Rouault, T. A., Harford, J. B., and Klausner, R. D. (1988) *J. Biol. Chem.* **263,** 19048–19052
65. Piccinelli, P., and Samuelsson, T. (2007) *Rna* **13,** 952–966
66. Weiss, M. J., Zhou, S., Feng, L., Gell, D. A., Mackay, J. P., Shi, Y., and Gow, A. J. (2005) *Ann. N. Y. Acad. Sci.* **1054,** 103–117
67. Schranzhofer, M., Schifrer, M., Cabrera, J. A., Kopp, S., Chiba, P., Beug, H., and Mullner, E. W. (2006) *Blood* **107,** 4159–4167
68. Yip, Y. K., Waks, M., and Beychok, S. (1972) *J. Biol. Chem.* **247,** 7237–7244
69. Ben-Bassat, I., Mozel, M., and Ramot, B. (1974) *Blood* **44,** 551–555